

## Article

# Experimental Proof of Concept for Using Hybrid Paper Based on Silver Nanowires, Cellulose and Poly(dimethylsiloxane) in Systems Dynamic Analysis and Healthcare Applications

Grzegorz Dzido <sup>1,\*</sup> , Krzysztof Piotrowski <sup>1</sup> , Piotr Sakiewicz <sup>2</sup> , Klaudiusz Gołombek <sup>3</sup> , Sonia Bańbuła <sup>4</sup>,  
Natalia Domagała <sup>4</sup>, Martyna Ratajczak <sup>4</sup>, Mateusz Kunert <sup>4</sup> and Agnieszka Ignaszewska <sup>4</sup>

<sup>1</sup> Department of Chemical Engineering and Process Design, Faculty of Chemistry, Silesian University of Technology, 44-100 Gliwice, Poland; krzysztof.piotrowski@polsl.pl

<sup>2</sup> Department of Engineering Materials and Biomaterials, Faculty of Mechanical Engineering, Silesian University of Technology, 44-100 Gliwice, Poland; piotr.sakiewicz@polsl.pl

<sup>3</sup> Materials Research Laboratory, Faculty of Mechanical Engineering, Silesian University of Technology, 44-100 Gliwice, Poland; klaudiusz.golombek@polsl.pl

<sup>4</sup> Faculty of Chemistry, Silesian University of Technology, 44-100 Gliwice, Poland; sb303743@student.polsl.pl (S.B.); nd303744@student.polsl.pl (N.D.); mr303746@student.polsl.pl (M.R.); mk303745@student.polsl.pl (M.K.); agniign311@student.polsl.pl (A.I.)

\* Correspondence: gdzido@polsl.pl

**Abstract:** The research results and evaluation of the applicability of the original composition of hybrid paper based on silver nanowires (AgNWs), cellulose pulp (CP), and carbon nanotubes (CNTs) are presented and discussed. The material tested was used to manufacture sensors for mechanical deformation resulting from external influences or related to human activity interactions. The sensors were fabricated using an AgNWs + CP suspension and additives by the vacuum filtration method. The substrate obtained was machined and then laminated with a layer of poly(dimethylsiloxane) (PDMS). The recorded responses to selected types of imposed mechanical interactions in the form of changes in the relative resistance of the sensor throughout the tests showed a close cause-and-effect relationship. The response of the tested systems when applying an alternating magnetic field was also observed. The results indicate that the proposed solutions can find application in the monitoring of mechanical interactions resulting from the dynamic behavior of physical objects, as well as derived from selected human vital functions.

**Keywords:** silver nanowires; hybrid paper; flexible electronics; strain sensor



**Citation:** Dzido, G.; Piotrowski, K.; Sakiewicz, P.; Gołombek, K.; Bańbuła, S.; Domagała, N.; Ratajczak, M.; Kunert, M.; Ignaszewska, A. Experimental Proof of Concept for Using Hybrid Paper Based on Silver Nanowires, Cellulose and Poly(dimethylsiloxane) in Systems Dynamic Analysis and Healthcare Applications. *Appl. Sci.* **2024**, *14*, 6783. <https://doi.org/10.3390/app14156783>

Academic Editors: Manuel Mariani and Francesca Brero

Received: 25 June 2024

Revised: 25 July 2024

Accepted: 31 July 2024

Published: 3 August 2024



**Copyright:** © 2024 by the authors. Licensee MDPI, Basel, Switzerland. This article is an open access article distributed under the terms and conditions of the Creative Commons Attribution (CC BY) license (<https://creativecommons.org/licenses/by/4.0/>).

## 1. Introduction

In recent years, intensive research has been aimed at using renewable materials to manufacture components for smart microelectronic applications. In particular, this concerns flexible electronic solutions. Substrates made of poly(ethylene terephthalate) (PET) [1], polyurethane [2], elastomers [3], poly(dimethylsiloxane) (PDMS) [4], polyimine [5] or fabrics [6] are used for this purpose. There has been a growing interest observed in the use of naturally occurring materials such as sponge [7], a composition of chitin and lignin [8], or cellulose [9] as substrates. Among the previously mentioned materials, cellulose is the most commonly used in the form of fibers [10] and nanofibers [11] based on which the substrate is formed. In the latter case, the substrate is characterized by improved transparency [12]. Filter paper [13] and coffee filters [14] are also frequently used materials for such technical solutions. Using cellulose ensures that forming the final product is easy with regards to shape formation and flexibility. Some other advantages can be negligible toxicity, uncomplicated disposal, and low weight. Due to its widespread availability and relatively low price, cellulose is a promising component for flexible electronic solutions. The limitation of cellulose is its low moisture and heat resistance, poor mechanical strength,

and low thermal and electrical conductivity. Therefore, as mentioned earlier, this material is often combined with some other components to eliminate or at least minimize the drawbacks. When combined with an electrically conductive material such as silver [15], copper nanowires [16], CNTs [17], graphene [18], electrically conductive polymers [19–21] or their compositions [22], new technical possibilities can result, which provide a broader application in the fabrication of advanced solutions for electro-smog protection [23], chemical species-based sensors and actuators [24,25], consumer electronics [26], low-temperature heat sources [27], or energy recovery solutions [28].

In the solutions mentioned above, cellulose can be used as a substrate onto which an electrically conductive material is applied in the form of conductive pathways. Depending on the product's subsequent application, the process can be carried out using drop, paint, spray, dip, print coating, or hand-drawing techniques [29]. In an alternative approach, the electrically conductive material is implemented directly into the pulp bulk structure during its manufacturing stage to form a so-called hybrid paper [30]. Products manufactured this way can also be laminated using appropriate polymer resins, such as PDMS [10]. This treatment makes it possible to provide electrical insulation, simultaneously improving the mechanical and functional properties of the hybrid paper obtained this way.

Among the many mechanical strain sensor technical solutions, a relatively small group are those based on cellulose (or its derivatives) and AgNWs [31]. In solutions of this type, the system's response to external tensions is converted into an electrical signal, processed and then recorded in the form of time-dependent changes in relative resistance. Resistance in the electroconductive areas used in sensors can change due to the following three mechanisms: crack propagation, tunnelling, and disconnection–reconnection [15]. The latter mechanism prevails when 1D-type materials such as AgNWs or CNTs are in use. These conductors overlap to form some conductive networks based on conductive paths. As a result of the superimposed forces, these paths can undergo reversible disconnections and reconnections, which are reflected in related changes in the sensor's resistance.

Owing to their unique and versatile properties, technical solutions based on hybrid paper can also be used to construct multi-functional sensors for temperature measurement [32] or proximity sensing [33]. Such multi-task sensors may also perform additional duties, such as heating [34] or functioning as actuators [35].

As mentioned, AgNWs are a frequently used electrically conductive material for manufacturing sensor substrates. This is due to, among other things, their excellent electrical and thermal conductivity, as well as their relatively low susceptibility to external influences. The synthesis routes for their manufacture are relatively well understood, allowing control over the size of the final product. It is also essential that the synthesis does not require the use of environmentally hazardous reagents or sophisticated apparatus. Therefore, this makes the material easy to fabricate under laboratory conditions.

Silver nanowires are manufactured using the polyol process, in which polyols [36] act as both a reducing agent for the nanomaterial precursor and as a solvent for the reaction substrates and synthesized products. Fabrication of the nanowires in question is possible using a stabilizing substance, polyvinylpyrrolidone (PVP), with different molecular weights. By selective adsorption on surfaces with the highest surface energy (1 0 0), PVP enables the preferential expansion of the surfaces (1 1 1) that constitute the main component of the terminal parts of the nanowire [37]. Additionally, the anisotropic growth of AgNWs can be intensified by the addition of so-called mediating substances. These are usually represented by chlorides of monovalent metals or those occurring in two oxidation levels. The addition of these substances provides the possibility of technological control on the formation of nanowires at the nucleation stage. Moreover, it enables the elimination of oxygen adsorbed on the expanding (1 1 1) planes of the nanowires.

A literature review indicated the need for more information on stress sensors based on substrates using a mixture of conductive material and a filler of renewable material for their construction. This observation opened the field for research into this issue to fill the observed gap. The research allowed an experimental assessment of the feasibility

of using a hybrid paper made from a mixture of silver nanowires, cellulose pulp, and PDMS resin to manufacture sensors that respond to external forces. The results showed that the proposed solution can be successfully applied to indicate the dynamic interactions occurring in engineering issues. In addition, it was demonstrated that the developed solution has the potential to analyze effects related to human life activity, which may find application in healthcare.

## 2. Materials and Methods

### 2.1. Chemicals and Materials

The following materials and reagents were used to manufacture the PH-based sensors: cellulose pulp (P.H. BLIK, Toruń, Poland), Sylgard 184 silicone resin (PDMS) (The Dow Chem. Comp., Midland, MI, USA), AgNO<sub>3</sub> silver nitrate p.a. (Chempur, Piekary Śl., Poland), ethylene glycol p.a. (Chempur, Piekary Śl., Poland), polyvinylpyrrolidone PVP K-30 p.d.a. (Carl Roth GmbH, Karlsruhe, Germany), polyvinylpyrrolidone PVP K-30 p.a. (Carl Roth GmbH, Karlsruhe, Germany), CuCl<sub>2</sub>·H<sub>2</sub>O p.a. (POCH, Gliwice, Poland), and multi-walled carbon nanotubes (CNTs), 1–10 μm in length (PlasmaChem GmbH, Berlin, Germany). The materials and reagents were used as produced by the manufacturer without further purification.

### 2.2. Characterization of Materials

The fabricated and applied nanomaterials and sensors were analyzed with respect to morphology details and surface elemental composition using scanning electron microscopy (SEM) and an EDS analyzer. An SEM microscope, Phenom ProX (ThermoFisher Scientific, Waltham, MA, USA), working at an accelerating voltage of 10 kV, and Zeiss Supra 35 (Oberkochen, Germany), working at an accelerating voltage of 7–20 kV, were used to examine the morphology of the fabricated materials. Elemental analysis was performed with an energy-dispersive X-ray (EDS) detector (Thermo Scientific™ EDX UltraDry, Waltham, MA, USA). The UV–Vis spectrograms of the silver nanowire synthesis products were recorded using a U-2800A spectrometer (Hitachi, Tokyo, Japan) in a 10 mm thick quartz cuvette in the 300–700 nm radiation range. Investigation of the crystalline phase was performed on a Seifert 3003TT (Agfa-Seifert, Mortsel, Belgium) diffractometer using Cu Kα radiation ( $\lambda = 0.1540598$  nm) in the  $2\theta$  range 30–70° with a step size of 0.05°.

### 2.3. Preparation of Silver Nanowires

The laboratory synthesis of silver nanowires used for the fabrication of hybrid paper-based sensors was carried out according to the polyol process, in which ethylene glycol is used as a reductant for the AgNWs precursor (AgNO<sub>3</sub>) and simultaneously as a solvent for all components of the reaction environment. To 200 mL of ethylene glycol, 0.603 g of the stabilizing agent, PVP, and 0.08 mL of 50 mM of CuCl<sub>2</sub> solution in ethylene glycol were added. The whole mixture was stirred in a 250 mL Erlenmeyer flask using a magnetic stirrer at a mixing rate of 200 rpm and heated up to 150 °C. Once the predetermined temperature level was reached, 0.594 g of silver nanowire precursor was added to the medium. After 50 min of continuous mixing, the flask's contents took on a silver-grey color, indicating that the nanowire synthesis was complete. The whole flask's contents were cooled down to room temperature and then separated using a Hermle Z36HK centrifuge (Hermle, Wehingen, Germany) at 4200 rpm. The collected precipitate was washed with DI water and recentrifuged. This operation was repeated five times. The AgNWs obtained were stored in an aqueous dispersion and used later in sensor preparation.

### 2.4. Preparation of Sensor

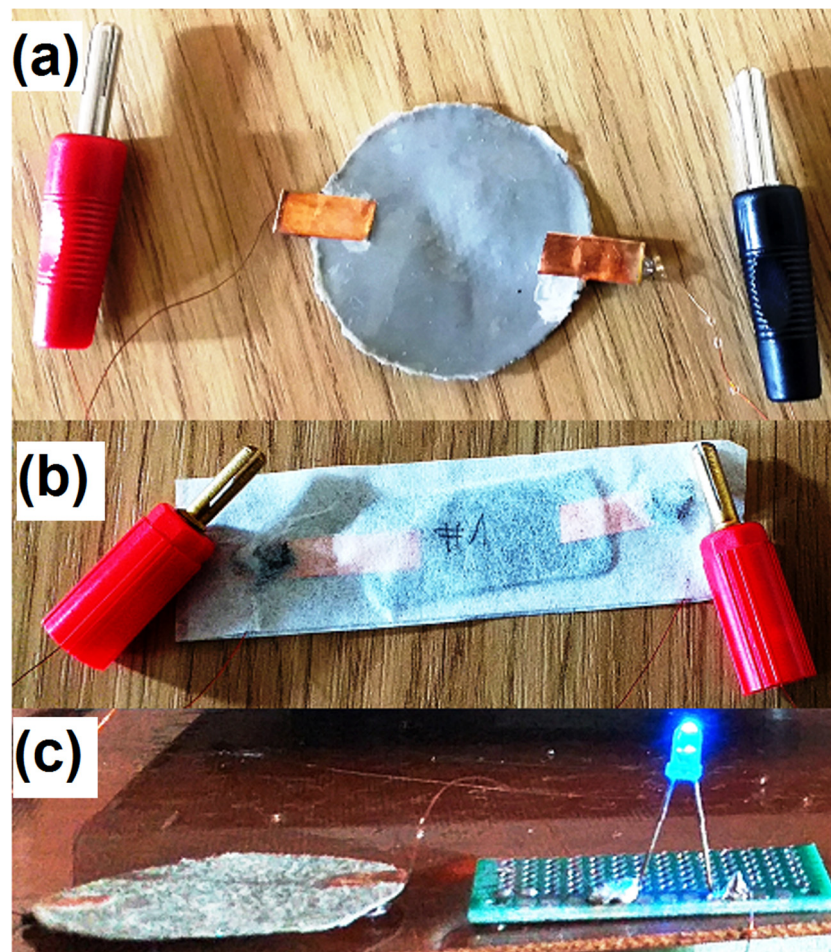
The sensors were fabricated using a modified methodology presented in [32]. A base suspension with 1% *w/w* cellulose was prepared by dispersing cellulose pulp in deionized water using a high shear rate mixer Micra D9 (Micra, Buggingen, Germany) for 30 min. The dispersion was then sonicated using an ultrasonic mixer (Sonics VCX-750, Newtown,

CT, USA) for 30 min at an oscillation amplitude of 65%. A measured volume of the CP suspension (20 mL) was mixed with a previously synthesized AgNWs dispersion at a concentration of  $0.043 \text{ g}_{\text{AgNWs}}/\text{mL}$ , sonicated for 3 min, and then separated from the host liquid using a vacuum filtration set on a 47 mm diameter hydrophilic PTFE filter with a pore diameter of  $0.45 \text{ }\mu\text{m}$  (Merck Millipore, Burlington, MA, USA). After the initial dehydration, the whole material was dried in a laboratory dryer at  $80 \text{ }^\circ\text{C}$  for 24 h. The material obtained was then compressed under a load of approximately 10,000 kg at room temperature. This procedure unifies and strengthens the structure of the manufactured raw hybrid paper and significantly improves the sensor's electrical conductivity. Subsequently, strips of copper sheets were glued to the sensor using a silver-based electrically conductive adhesive, and a 0.1 mm insulated copper wire connected to banana plugs was soldered. The stability and reliability of these connections are critical to the accuracy and reproducibility of the test results.

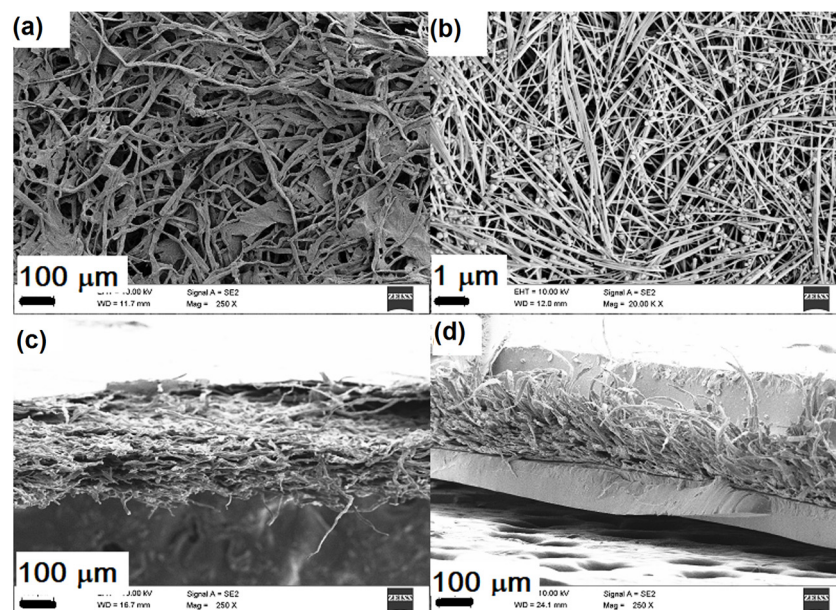
To avoid the potential effects of moisture on the measurement results and to increase the mechanical strength, the sensor was coated with PDMS resin with a crosslinking agent added beforehand. The entire assembly was cured at  $65 \text{ }^\circ\text{C}$  for 24 h. Covering the sensor with resin is particularly important when working in contact with the human body or monitoring respiratory activity. The insulation prevents the influence of sweat or high moisture content in exhaled air on the test item's readings and functioning. Other authors have shown that temperature changes can also affect the results obtained with sensors of a similar design [32]. However, given the relatively small range of variations in human body temperature, this effect can be neglected, especially when high-precision readings are not required. The sensors used in this study had a silver nanowire content of (#1)  $0.325 \text{ g}_{\text{AgNWs}}/\text{g}_{\text{CP}}$ , (#2)  $0.182 \text{ g}_{\text{AgNWs}}/\text{g}_{\text{CP}}$ , (#3)  $0.092 \text{ g}_{\text{AgNWs}}/\text{g}_{\text{CP}}$ , and (#4)  $0.645 \text{ g}_{\text{AgNWs}}/\text{g}_{\text{CP}}$ . For sample #5 containing  $0.325 \text{ g}_{\text{AgNWs}}/\text{g}_{\text{CP}}$ , 0.02 g of carbon nanotubes was added during the slurry formation stage, resulting in a concentration of approximately  $0.1 \text{ g}_{\text{CNTs}}/\text{g}_{\text{CP}}$ . Five samples were prepared according to the procedure described. Each was used twice. Examples are shown in Figure 1. For the tests involving mechanical interactions, such as applying a weight, tapping the surface with a finger and magnetic field interactions, untreated sensors were used, as shown in Figure 1a. The form shown is, however, inconvenient for experiments involving human participation. Therefore, after the appropriate trimming and combining with medical plaster, the sensors, as shown in Figure 1b, were used to study human reflexes (swallowing, speaking words, twisting the neck, bending the finger) and imaging damped vibrations. It is worth mentioning that the shape modification used did not significantly affect the functional properties of the sensors tested. Figure 1c shows the selected sensor in an electric circuit with an LED and DC supply.

Figure 2 shows SEM images of the components used in the construction of the sensors and a cross-section of the selected item. Figure 2a illustrates the cellulose pulp sample used in the study with an average diameter of 20–50  $\mu\text{m}$ . The silver nanowires applied in the study are shown in Figure 2b. The cross-section of the hybrid paper before coating with PDMS resin is depicted in Figure 2c. The average width of the structure in question is approximately 120  $\mu\text{m}$ . After coating both sides with PDMS resin, the thickness of the sensor increased up to approximately 350  $\mu\text{m}$  (Figure 2d).

Figure 3a,b show the hybrid paper's opposite surfaces before applying the resin layer. Surprisingly, the distribution of the AgNWs layer is asymmetric despite the intensive mixing of the nanowire and cellulose suspension during the application to the filter surface. The observed stratification structure results from the differences in density and size of AgNWs compared to cellulose pulp fibers. A similar effect was not observed in other available research data when cellulose nanofibers were applied [12,17]. Thus, it may represent a technological constraint in some applications of this type of sensor, especially when material transparency is expected. Using a connection that covered both sides of the sensor minimized the possible effect of asymmetrical conductor distribution.



**Figure 1.** Examples of the original hybrid paper-based sensor fabrications for studies on: (a) mechanical interactions between sensor and strain forcing object, sample #2, (b) human vital reflexes, sample #1, (c) sensor—LED—DC power supply circuit connection.



**Figure 2.** SEM images representing samples of: (a) cellulose pulp, (b) prepared silver nanowires, (c) hybrid paper cross-section, (d) hybrid paper coated on both sides with PDMS resin.

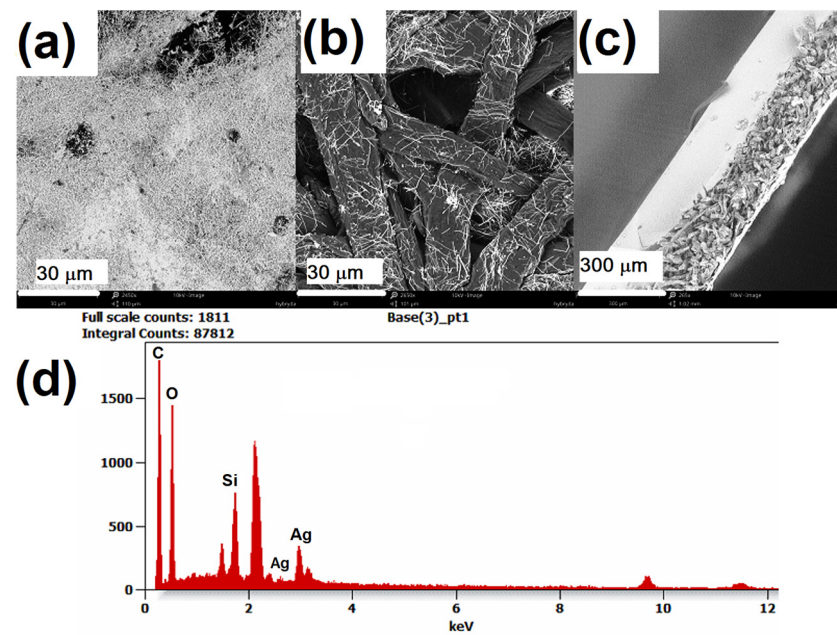


**Figure 3.** SEM images showing: (a,b) opposite surfaces of a single sensor, (c) cross-section of a single sensor, (d) EDX of the sensor material cross-section surface.

It is worth mentioning that both surfaces of the hybrid paper, despite differences in silver nanowire coating, showed electrical conductivity during the simple measurements using a typical ohmmeter. Figure 3c illustrates a cross-sectional view of a sensor, with only one side coated with resin. It allows one to estimate the approximate thickness of the AgNWs layer to be approximately 10  $\mu\text{m}$ . Elemental EDS analysis of the cross-section confirmed the presence of elements in the components used to fabricate the sensor (Figure 3d). This concerns, in particular, the carbon and oxygen atoms that make up the substrate, the silver that forms the electroconductive layer, and the silicon, which, in addition to oxygen and carbon, is part of the PDMS silicone resin.

### 2.5. Testing of Fabricated Sensors

A measurement system, whose schematic diagram is shown in Figure 4, was used to test the properties of the sensors fabricated on the base of the hybrid paper.

This circuit used a laboratory DC power supply (Stamos, S-LS-32, Berlin, Germany) as the external electricity source. The electric current flowing through the sensor under test and a resistor with a resistance of  $R_r = 1 \text{ Ohm}$  induced voltage drops of  $\Delta U_1$  and  $\Delta U_2$ , respectively. The voltage drops were measured using an analogue-to-digital converter (Advantech 4716, Taipei, Taiwan), transferred to a computer, and saved as an Excel<sup>®</sup> data format. Knowledge of the voltage drop  $\Delta U_2$  enabled the magnitude of the electrical current conducted through the system to be determined based on Ohm's law  $I = \Delta U_2/R_r$ . The current value of the electrical resistance and its relative change  $\Delta R/R_0$  for the test sample were calculated as (1) and (2):

$$R = \frac{\Delta U_1}{I} \quad (1)$$

$$\frac{\Delta R}{R_0} = \frac{R - R_0}{R_0} \quad (2)$$

where  $R_0$ —initial resistance of the sensor, and  $R$ —instantaneous value of resistance of the sensor determined during the experiment run.

Measurements were performed at sampling frequencies of 100 and 1000 Hz, and at a supply voltage of 0.15 V. This minimized the supply's influence on the  $\Delta R$  value and ensured safety in direct contact with the sensor system.

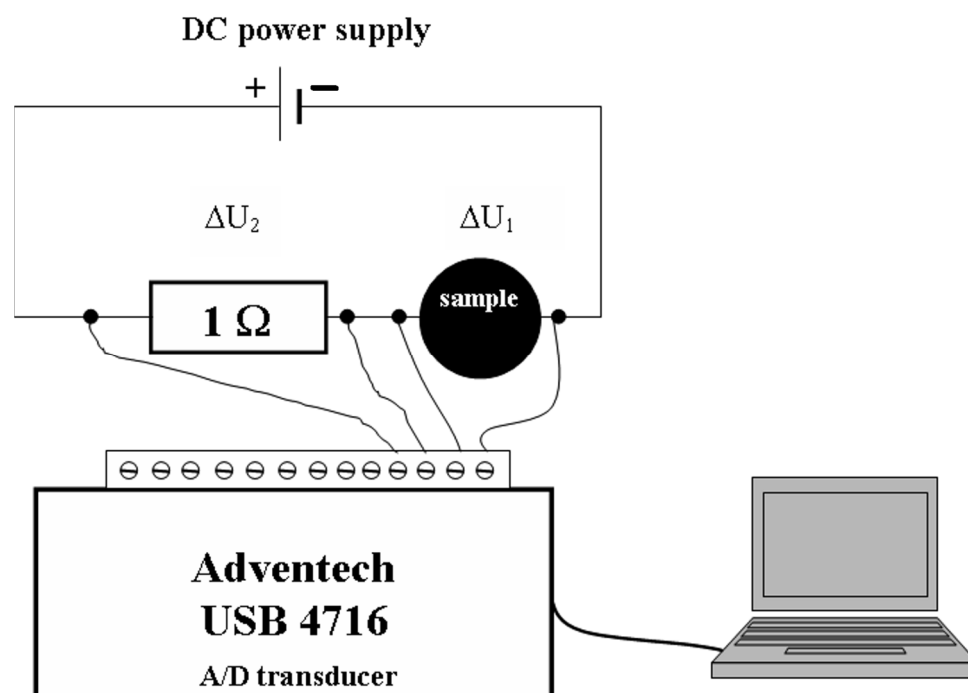


**Figure 4.** Schematic diagram of the electrical system for hybrid paper sensor research.

Passive and active mechanical interaction scenarios were carried out to determine the performance properties of the tested sensors. In the former case, the sensor was cyclically loaded and unloaded. In the latter case, the tensions generated resulted from tapping the sensor's surface, whereas damped vibrations or interactions resulted from typical human activities. The cyclic changes implemented during the measurements also made it possible to analyze combinations of the interactions mentioned earlier. The tests also identified the effect of an alternating magnetic field on the recorded  $\Delta R/R_0$  vs. time courses. During the experiments, the state of the test material, without any interactions and as the reference level, was recorded for the first 20 s of the measurement to assess the influence of electrical interference on the experimental results. All measurements were carried out in a room or at the human body temperature.

### 3. Results and Discussion

#### 3.1. Characterization of the Synthesized Silver Nanowires

The silver nanowires used in the study are shown in Figure 2b. The average diameter of the nanomaterials was 80–120 nm, while the length varied between 10 and 30  $\mu\text{m}$ . It is also possible to observe inclusions in the silver crystallites with a morphology that differs from that of the expected 1D objects. However, the practical effect of such objects on electrical conductivity, based on the authors' observations, is negligible.

X-ray diffraction (XRD) analysis was used to evaluate the structure of the selected sample of AgNWs. Figure 5a shows a typical XRD spectrum for the manufactured AgNWs. Diffraction peaks occurring at  $2\Theta = 38.10, 44.25$  and  $64.35^\circ$  are in line with the peaks which describe bulk silver (ICSD card No. 01-071-6549). They can be attributed to the crystallographic (111), (200), and (220) planes of face-centered cubic silver crystals. The observed (111) to (200) intensity of the reflexes ratio amounts to 3.7 (Figure 5a), and it surpasses the theoretical value of 2.2 (ICSD sheet No. 01-071-6549). The value indicates a significant quantity of the (111) crystal planes in the sample analyzed and a favored direction of growth of one-dimensional silver nanostructures [38].

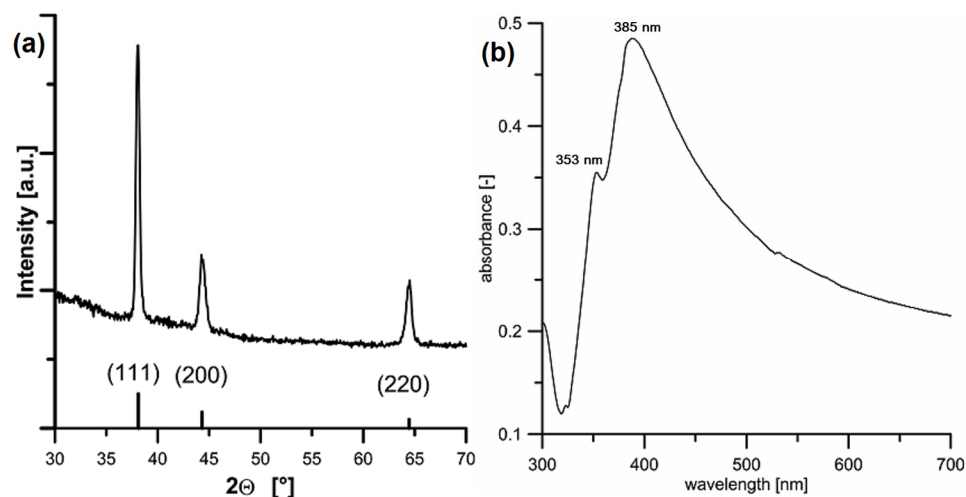


Figure 5. Spectra of the synthesized silver nanowires: (a) XRD spectrum, (b) UV-Vis spectrum.

Figure 5b shows the UV-Vis spectrogram obtained for the AgNWs dispersion used to manufacture the sensors. The observed maximum at around 385 nm and the shoulder peak at 351 nm correspond to the transverse surface plasmon resonance of AgNWs. The absence of a maximum for wavelengths above 400 nm indicates the absence of nanoparticles in the suspension studied [39].

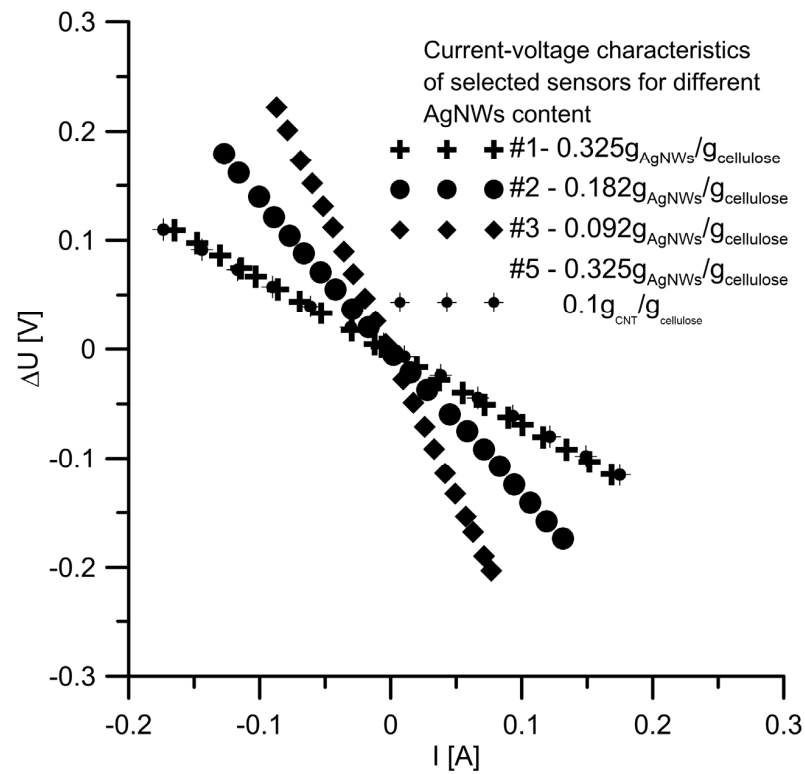
### 3.2. Test Results with Hybrid Paper-Based Sensors

The prepared sensors were tested to assess their suitability for indicating dynamic strains resulting from mechanical activity, as well as effects related to the functioning of the human body. Figure 6 illustrates the investigated sensors' current-voltage (U-I) characteristics for different contents of the AgNWs. A characteristic linear course was recorded in all cases, indicating that Ohm's law was strictly satisfied for the experimental range tested. For the cases presented, the calculated coefficient of determination  $R^2$  was 0.999. As expected, the slopes of the straight lines, and therefore the electrical resistances of the tested samples, increase proportionally with a decrease in the concentration of the AgNWs used. In the case of sample #5, the added CNTs had no significant effect on the U-I characteristics, which do not differ significantly from those observed for reference sample #1. It is probably due to differences in the lengths of the CNTs and the fabricated AgNWs. Silver nanowires, being longer, are easier to form a conductive path with. Hence, nanowires' dominant influence on the sensors' electric conductivity mechanism was confirmed experimentally. The rectilinear course of the characteristics of all investigated samples also allows one to conclude that the influence of the thermal effect caused by the flow of electric current through the sensor is negligibly small. During the tests, instantaneous changes in the relative resistance of the sensors were observed, especially within the  $-15$  up to  $+160\%$  range.

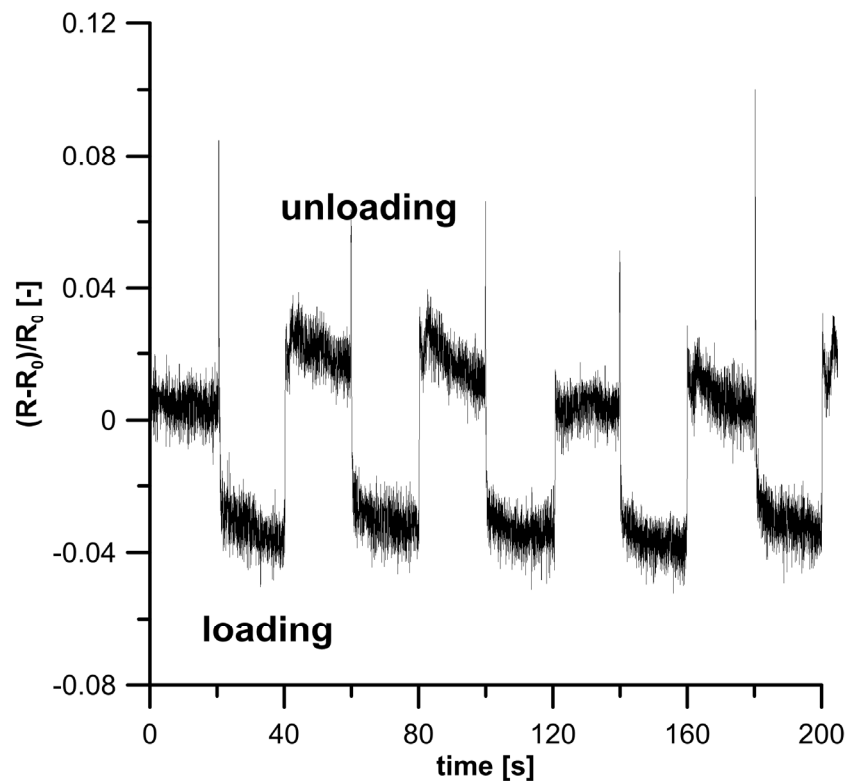
Figure 7 illustrates the response of the test system resulting from the cyclic loading and unloading of a 200 g weight onto the surface of sensor #1. After loading the weight, it remained on the sample surface for 20 s. A good representation of the forced activity waveform can be observed. The peaks observed in Figure 7 immediately after applying the weight are probably related to the dynamic deformation of the PDMS layer, which is then transferred to the hybrid paper substrate. In this situation, the hypothesis of an electro-tribological effect cannot be rejected either. However, this requires further experimental validation. After the test specimen is loaded or unloaded, a slight, progressive change in specific resistance of 0.02 is observed over time, caused by the gradual micro-deformation of the tested material. The recorded run indicates a relatively short response time duration. The problem is the results' repeatability, especially the return to starting reference conditions after the mechanical impulse has ceased. However, this does not exclude the possibility of



using the sensor in question to indicate simple mechanical impacts, especially at low rates of change.

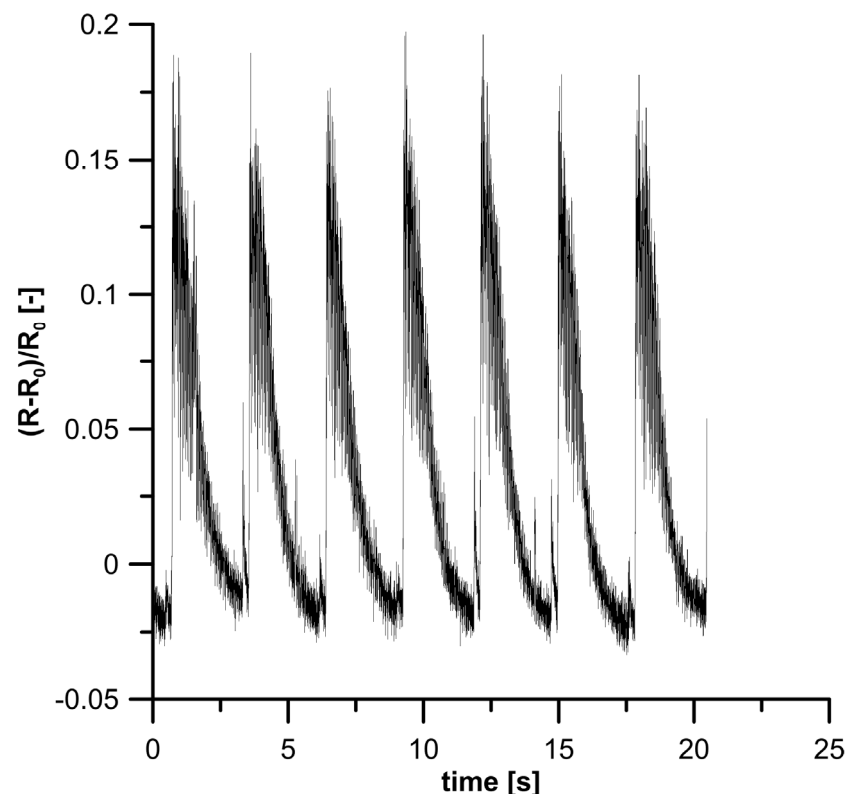


**Figure 6.** Current–voltage characteristics of AgNWs-based sensors made on hybrid paper for different conductor materials concentrations.



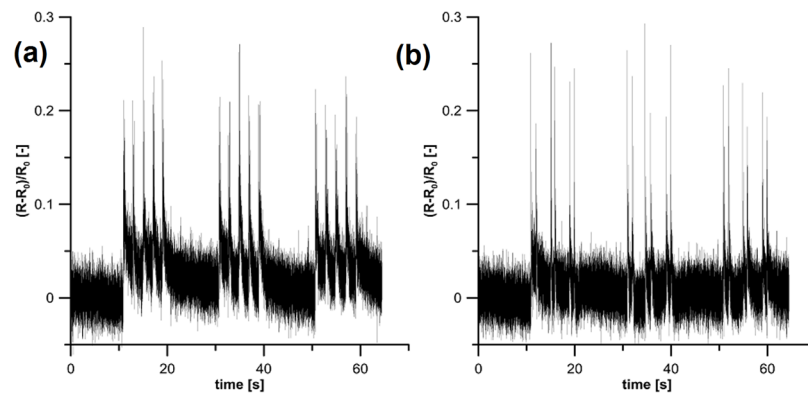
**Figure 7.** Effect of cyclic loading and unloading of sensor #1 using a 200 g weight.

Figure 8 shows the recorded results of the mechanical stimulation of a flexible element on which surface the sensor was attached. The mechanical perturbations were induced by a metal rod attached to the shaft of a DC motor spinning at a frequency of approximately 0.35 Hz. The applied unit pulse induced intense vibrations, which then quickly disappeared. The sampling frequency of the signal equal to 1000 Hz was then used to represent the acquired response more clearly. The recorded waveforms are due to inertial forces occurring during damped oscillations and are in line with the observations of other authors [32]. In the case studied, good repeatability of the recorded results was observed. Similar results from this part of the study can be used in the future to analyze the dynamic behavior of the systems studied.



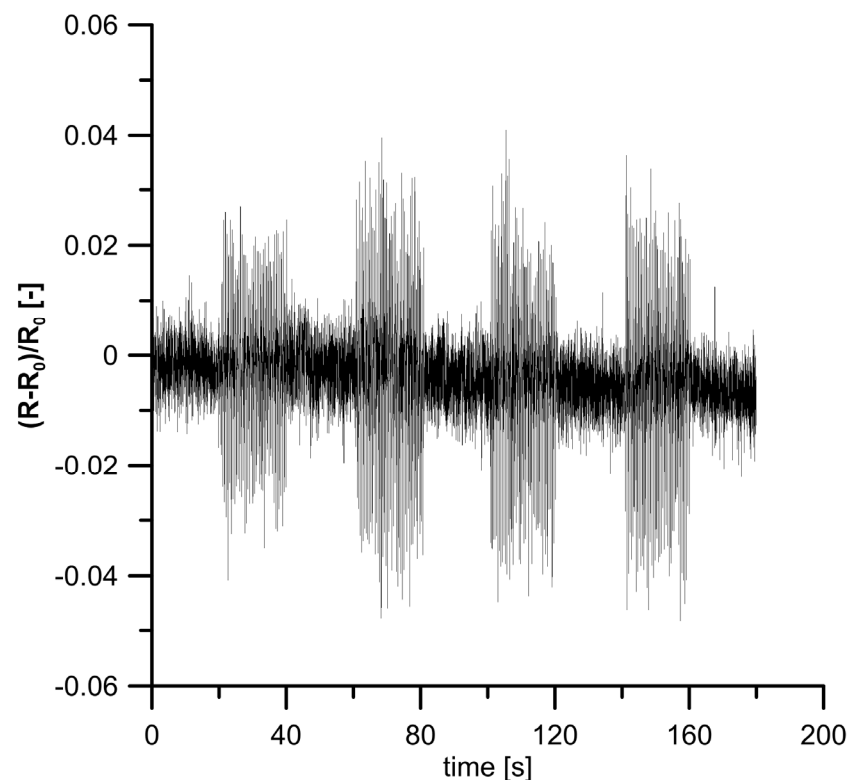
**Figure 8.** Response curve of periodical mechanical stimulation of sample #3 at a frequency of about 0.35 Hz. Signal sampling frequency 1000 Hz.

Figure 9 shows the effect of cyclic finger pressure on sensor #4, implemented according to two scenarios. In the first scenario, the sensor was pressed twice within one second (Figure 9a). It was followed by a two-second pause, after which the experimental procedure was repeated. In the second scenario, the sensor was acted upon in a cycle of one press every second, followed by a two-second pause (Figure 9b). In all cases, the measurement series were separated by a time interval of 10 s, during which the sensor was not touched at all. Using a sampling frequency of 1000 Hz gave satisfactory reproduction of the assumed pattern. The result indicates that advanced mechanical interaction patterns can be recorded for the presented measurement system based on a hybrid paper solution. The inspiration for this type of experiment was an attempt to imitate normal heart sounds. At this stage of the work, attempts to record the heart rate using sensors stabilized on the wrist or neck, however, did not yield some satisfactory and repeatable effects. This results from the intensity of the forcing pulse being too low compared to the noise and interferences observed in the measurement system.



**Figure 9.** Cyclic mechanical interaction with finger; sample #4: (a) first scenario, (b) second scenario. Signal sampling frequency of 1000 Hz.

An interesting effect was observed when the neodymium magnet was cycled over the sensor surface (Figure 10). A small in magnitude but measurable change in the relative resistance of the sensor in an alternating magnetic field could be observed. It may be attributed to the generation of additional electric current within the system, which is the result of the changes in the magnetic field intensity caused by the magnet's periodical movement. This effect is superimposed on the constant component, resulting from the flow of constant current underlying the operation of the test system. It is worth mentioning that other authors observed a similar effect of an external magnetic field on the properties of a sensor made of a magneto-rheological elastomer [2]. This observed phenomenon may provide a basis for the design of cost-effective and non-contact displacement sensors.



**Figure 10.** Effect of alternating strong magnetic field on sample #3.

In addition to typical tests showing the possible applications of the developed sensors for inanimate physical objects, additional studies were carried out that confirmed the

applicability of the hybrid paper-based sensor system for health monitoring purposes. Figure 11a illustrates using a sensor stabilized on the index finger, which was bent cyclically.

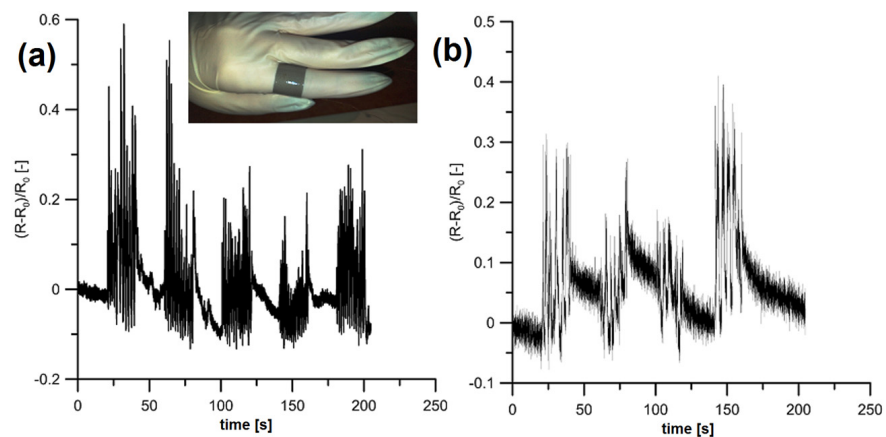


**Figure 11.** Effect of selected vital activities: (a) cyclic bending of the finger (sample #2), (b) blowing on the flat sensor (sample #5) surface by the test participant.

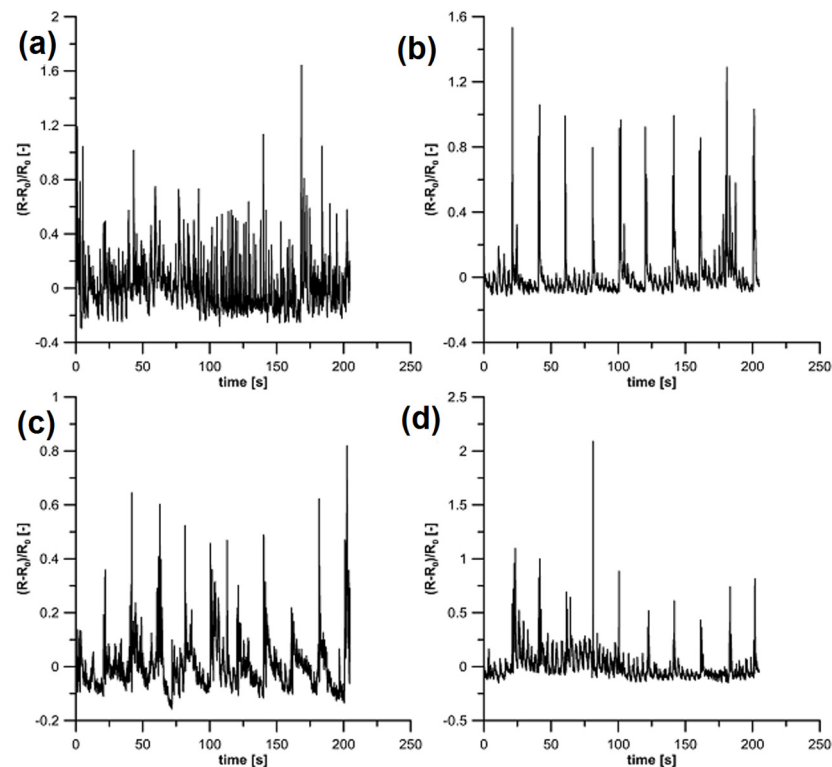
A clear relationship between the recorded signal and the applied forcing can be observed. Figure 11b portrays the effect of air blown out of the mouth, perpendicular to the sensor surface, on its response. The experiment was repeated recurrently for different intensities of exhaled air. The courses presented give a reasonable indication of the activities carried out, while the correct interpretation of the signals obtained remains an open question.

Figure 12 shows the signals measured with the sensor stabilized on the surface of the neck. In order to compare the effect achieved in the first stage, the signal was recorded in the absence of activity (Figure 12a). Random and chaotic signal runs are likely the result of electrical noise generated in the measurement system and mechanical disturbances characteristic of the sensor's location resulting from human activity. The following runs show the response of the system to physiological actions, such as pronouncing alphabet letters aloud (Figure 12b), swallowing (Figure 12c), and head turns (Figure 12d). Some clear correlation between the activities performed and the recorded courses can be observed, which differs significantly from the previously recorded background. Furthermore, slight differences can be found between the courses obtained for the individual activities.

The recorded courses, presented in Figures 11 and 12, are characterized by limited repeatability and stability. It can be attributed to the realization of experiments involving a human being whose presence introduces additional, unexpected disturbances. As a result, conditions close to those found in everyday life are obtained.

The proper interpretation of the observed effects and differences requires using signal analysis with the application of advanced mathematical tools, such as artificial neural networks, and it will be the subject of future authors' works.

At the present research stage, it is still rather early to distinguish the most suitable solution in terms of the content of the electrically conductive material. It is primarily dictated by the intended application of the sensor and the associated type and magnitude of interacting forces. The absence of the electroconductive material or its use in a pure, homogeneous form leads to a lack of response in the measurement system. It can therefore be assumed that there is a certain optimum amount of AgNWs for a given mechanical interaction and application. The use of CNTs did not show an additional improvement in sensor properties. Nevertheless, it can be expected that the AgNWs–CNTs composition can provide a long life cycle when using such a material, as suggested by other authors [23].



**Figure 12.** Response curves of physiological reflexes recorded with hybrid paper-based sensor—sample #3: (a) lack of activity, (b) pronouncing consecutive letters, (c) swallowing, (d) alternating head turns.

#### 4. Conclusions

The conducted research on the manufacture and application of original technical sensor solutions involving hybrid paper based on silver nanowires showed the excellent application potential of this material for the manufacture of sensors of mechanical interactions with a particular focus on health-promoting solutions. A significant effect of an alternating magnetic field on the recorded results was found, which opens space up for further research into new applications of the sensors in question. The results also made it possible to identify the main drawbacks of the proposed solution concerning the manufacturing methodology and repeatability of results. Removal of the demonstrated problems will be the goal of further authors' research. Further work is also required to design and develop algorithms for acquiring, processing, and interpreting the output signal in the effective transducer.

**Author Contributions:** G.D. methodology, conceptualization, software, writing—review and editing; K.P. methodology, formal analysis, writing—review and editing; P.S. formal analysis, writing—original draft preparation; K.G. formal analysis, original draft preparation, visualization; S.B. investigation, visualization, data curation; N.D. investigation, visualization, data curation; M.R. investigation, visualization, data curation; M.K. investigation, visualization, data curation; A.I. investigation, visualization, data curation. All authors have read and agreed to the published version of the manuscript.

**Funding:** The research was carried out as a result of a student educational research project within the 10th edition (2023/2024) of Project Based Learning (PBL) under the program “Silesian University of Technology as a center for modern education based on research and innovation”.

**Institutional Review Board Statement:** Not applicable.

**Informed Consent Statement:** Not applicable.

**Data Availability Statement:** The raw data supporting the conclusions of this article will be made available by the corresponding author on request.

**Acknowledgments:** The authors would also like to thank Alicja Kazek-Kęsik for her assistance in preparing and interpreting XRD spectrograms.

**Conflicts of Interest:** The authors declare no conflicts of interest.

## References

1. Zhao, L.; Qiao, J.; Li, F.; Yuan, D.; Huang, J.; Wang, M.; Xu, S. Laser-patterned hierarchical aligned micro-/nanowire network for highly sensitive multidimensional strain sensor. *ACS Appl. Mater. Interfaces* **2022**, *14*, 48276–48284. [[CrossRef](#)] [[PubMed](#)]
2. Hu, T.; Xuan, S.; Ding, L.; Gong, X. Stretchable and magneto-sensitive strain sensor based on silver nanowire-polyurethane sponge enhanced magnetorheological elastomer. *Mater. Des.* **2018**, *156*, 528–537. [[CrossRef](#)]
3. Kim, K.H.; Jang, N.S.; Ha, S.H.; Cho, J.H.; Kim, J.M. Highly sensitive and stretchable resistive strain sensors based on microstructured metal nanowire/elastomer composite films. *Small* **2018**, *14*, 1704232. [[CrossRef](#)] [[PubMed](#)]
4. Li, W.; He, Y.; Xu, J.; Wang, W.; Zhu, Z.; Liu, H. Preparation of Ag NWs and Ag NWs@PDMS stretchable sensors based on rapid polyol method and semi-dry process. *J. Alloys Comp.* **2019**, *803*, 332–340. [[CrossRef](#)]
5. Wang, Y.; Chen, Q.; Zhang, G.; Xiao, C.; Wei, Y.; Li, W. Ultrathin flexible transparent composite electrode via semiembedding silver nanowires in a colorless polyimide for high performance ultraflexible organic solar cells. *ACS Appl. Mater. Interfaces* **2022**, *14*, 5699–5708. [[CrossRef](#)]
6. Repon, R.; Mikucioniene, D. Progress in flexible electronic textile for heating application: A critical review. *Materials* **2021**, *14*, 6540. [[CrossRef](#)]
7. Dong, X.; Wei, Y.; Chen, S.; Lin, Y.; Liu, L.; Li, Y. A linear and large-range pressure sensor based on a graphene/silver nanowires nanobiocomposites network and a hierarchical structural sponge. *Compos. Sci. Technol.* **2018**, *155*, 108–116. [[CrossRef](#)]
8. Kwon, Y.B.; Kim, J.H.; Kim, Y.K. Efficient protection of silver nanowire transparent electrodes by all-biorenewable layer-by-layer assembled thin films. *ACS Appl. Mater. Interfaces* **2022**, *14*, 25993–26003. [[CrossRef](#)]
9. Teodoro, K.B.R.; Sanfelice, R.C.; Migliorini, F.L.; Pavinatto, A.; Facure, M.H.M.; Correa, D.S. A review on the role and performance of cellulose nanomaterials in sensors. *ACS Sens.* **2021**, *6*, 2473–2496. [[CrossRef](#)] [[PubMed](#)]
10. Zhu, M.; Yan, X.; Lei, Y.; Guo, J.; Xu, Y.; Xu, H.; Dai, L.; Kong, L. An ultrastrong and antibacterial silver nanowire/aligned cellulose scaffold composite film for electromagnetic interference shielding. *ACS Appl. Mater. Interfaces* **2022**, *14*, 14520–14531. [[CrossRef](#)]
11. Han, M.; Shen, W.; Tong, X.; Corriou, J.P. Cellulose nanofiber/MXene/AgNWs composite nanopaper with mechanical robustness for high-performance humidity sensor and smart actuator. *Sens. Actuators B Chem.* **2024**, *406*, 135375. [[CrossRef](#)]
12. Koga, H.; Nogi, M.; Komoda, N.; Nge, T.T.; Sugahara, T.; Suganuma, K. Uniformly connected conductive networks on cellulose nanofiber paper for transparent paper electronics. *NPG Asia Mater.* **2014**, *6*, e93. [[CrossRef](#)]
13. Shobin, L.R.; Manivannan, S. Silver nanowires-single walled carbon nanotubes heterostructure chemiresistors. *Sens. Actuators B* **2018**, *256*, 7–17. [[CrossRef](#)]
14. Chen, Y.C.; Hsu, J.H.; Lin, Y.G.; Hsu, Y.K. Silver nanowires on coffee filter as dual-sensing functionality for efficient and low-cost SERS substrate and electrochemical detection. *Sens. Actuators B* **2017**, *245*, 189–195. [[CrossRef](#)]
15. Raman, S.; Arunagirinathan, R.S. Silver nanowires in stretchable resistive strain sensors. *Nanomaterials* **2022**, *12*, 1932. [[CrossRef](#)]
16. Li, Z.; Chang, S.; Khuje, S.; Ren, S. Recent advancement of emerging nano copper-based printable flexible hybrid electronics. *ACS Nano* **2021**, *15*, 6211–6232. [[CrossRef](#)]
17. Kang, K.; Lin, M.F.; Chen, J.; Lee, P.S. Highly transparent conducting nanopaper for solid state foldable electrochromic devices. *Small* **2016**, *12*, 6370–6377. [[CrossRef](#)] [[PubMed](#)]
18. Ferrero, G.A.; Sevilla, M.; Fuertes, A.B. Free-standing hybrid films based on graphene and porous carbon particles for flexible supercapacitors. *Sust. Energy Fuels* **2017**, *1*, 127–137. [[CrossRef](#)]
19. Yang, S.; Qian, X. Conductive PPy@cellulosic paper hybrid electrodes with a redox active dopant for high capacitance and cycling stability. *Polymers* **2022**, *14*, 2634. [[CrossRef](#)]
20. Köwitsch, A.; Zhou, G.; Growth, T. Medical application of glycosaminoglycans: A review. *J. Tissue Eng. Regen. Med.* **2017**, *12*, 23–41. [[CrossRef](#)]
21. Gao, G.; Edgar, K.J. Efficient synthesis of glycosaminoglycan analogs. *Biomacromolecules* **2019**, *20*, 608–617. [[CrossRef](#)] [[PubMed](#)]
22. Cao, Y.; Lai, T.; Teng, F.; Liu, C.; Li, A. Highly stretchable and sensitive strain sensor based on silver nanowires/carbon nanotubes on hair band for human motion detection. *Prog. Nat. Sci. Mat. Int.* **2021**, *31*, 379–386. [[CrossRef](#)]
23. Choi, H.Y.; Lee, T.W.; Lee, S.E.; Lim, J.D.; Leong, Y.G. Silver nanowire/carbon nanotube/cellulose hybrid papers for electrically conductive and electromagnetic interference shielding elements. *Compos. Sci. Technol.* **2017**, *150*, 45–53. [[CrossRef](#)]
24. Huang, L.; Jiang, P.; Wang, D.; Luo, Y.; Li, M.; Lee, H.; Gerhardt, R.A. A novel paper-based flexible ammonia gas sensor via silver and SWNT-PABS inkjet printing. *Sens. Actuators B* **2014**, *197*, 308–313. [[CrossRef](#)]
25. Yao, S.; Cui, J.; Cui, Z.; Zhu, Y. Soft electrothermal actuators using silver nanowire heaters. *Nanoscale* **2017**, *9*, 3797–3805. [[CrossRef](#)] [[PubMed](#)]
26. Barras, R.; Cunha, I.; Gaspar, D.; Fortunato, E.; Martins, R.; Pereira, L. Printable cellulose-based electroconductive composites for sensing elements in paper electronics. *Flex. Print. Electron.* **2017**, *2*, 014006. [[CrossRef](#)]

27. Cheng, R.; Wang, B.; Zeng, J.; Li, J.; Xu, J.; Gao, W.; Chen, K. High-performance and rapid-response electrical heaters derived from cellulose nanofiber/silver nanowire nanopapers for portable thermal management. *ACS Appl. Mater. Interfaces* **2022**, *14*, 30144–30159. [[CrossRef](#)]
28. Bańbuła, S.; Domagała, N.; Ratajczak, M.; Kunert, M.; Ignaszewska, A.; Dzido, G.; Piotrowski, K.; Sakiewicz, P. Experimental proof-of-concept application of a triboelectric nanogenerator using a single polymer composite electrode for monitoring environmental factors. In Proceedings of the Contemporary Environmental and Energy Problems, Gliwice, Poland, 18–21 September 2023; *in press*.
29. Tai, T.; Duan, Z.; Wang, Y.; Wang, S.; Jiang, Y. Paper-based sensors for gas, humidity, and strain detections: A review. *ACS Appl. Mater. Interfaces* **2020**, *12*, 31037–31053. [[CrossRef](#)]
30. Betker, M.; Harder, C.; Erbes, E.; Heger, J.E.; Alexakis, A.E.; Sochor, B.; Chen, Q.; Schwartzkopf, M.; Körstgens, V.; Müller-Buschbaum, P.; et al. Sprayed hybrid cellulose nanofibril–silver nanowire transparent electrodes for organic electronic applications. *ACS Appl. Nano Mater.* **2023**, *6*, 13677–13688. [[CrossRef](#)]
31. Cheng, R.; Zeng, J.; Wang, B.; Li, J.; Cheng, Z.; Xu, J.; Gao, W.; Chen, K. Ultralight, flexible and conductive silver nanowire/nanofibrillated cellulose aerogel for multifunctional strain sensor. *Chem. Eng. J.* **2021**, *424*, 130565. [[CrossRef](#)]
32. Yin, R.; Yang, S.; Li, Q.; Zhang, S.; Liu, H.; Han, J.; Liu, C. Flexible conductive Ag nanowire/cellulose nanofibril hybrid nanopaper for strain and temperature sensing applications. *Sci. Bull.* **2020**, *65*, 899–908. [[CrossRef](#)] [[PubMed](#)]
33. Guan, F.; Xie, Y.; Wu, H.; Meng, Y.; Shi, Y.; Gao, M.; Zhang, Z.; Chen, S.; Chen, Y.; Wang, H.; et al. Silver nanowire–bacterial cellulose composite fiber-based sensor for highly sensitive detection of pressure and proximity. *ACS Nano* **2020**, *14*, 15428–15439. [[CrossRef](#)] [[PubMed](#)]
34. Han, J.W.; Prameswari, A.; Entifar, S.A.N.; Kim, J.H.; Wibowo, A.F.; Park, J.; Lee, J.; Kim, S.; Lim, D.C.; Moon, M.W.; et al. Highly conductive, flexible, and robust silver nanowire-embedded carboxymethyl cellulose/poly(3,4-ethylenedioxythiophene):poly(styrenesulfonate) composite films for wearable heaters and on-skin sensors. *Electron. Mat. Lett.* **2022**, *18*, 532–539. [[CrossRef](#)]
35. Kumar, K.S.; Zhang, L.; Kalairaj, M.S.; Banerjee, H.; Xiao, X.; Jiayi, C.C.; Huang, H.; Lim, C.M.; Ouyang, J.; Ren, H. Stretchable and sensitive silver nanowire-hydrogel strain sensors for proprioceptive actuation. *ACS Appl. Mater. Interfaces* **2021**, *13*, 37816–37829. [[CrossRef](#)] [[PubMed](#)]
36. Dzido, G.; Smolska, A.; Farooq, M.O. Rapid synthesis of silver nanowires in the polyol process with conventional and microwave heating. *Appl. Sci.* **2023**, *13*, 4963. [[CrossRef](#)]
37. Wiley, B.; Sun, Y.; Xia, Y. Polyol synthesis of silver nanostructures: Control of product morphology with Fe(II) or Fe(III) species. *Langmuir* **2005**, *21*, 8078–8080. [[CrossRef](#)]
38. Luu, Q.N.; Doorn, J.M.; Berry, M.T.; Jiang, C.; Lin, C.; May, P.S. Preparation and optical properties of silver nanowires and silver-nanowire thin films. *J. Colloid Interface Sci.* **2011**, *356*, 151–158. [[CrossRef](#)]
39. Mao, H.; Feng, J.; Ma, X.; Wu, C.; Zhao, X. One-dimensional silver nanowires synthesized by self-seeding polyol process. *J. Nanopart. Res.* **2012**, *14*, 887. [[CrossRef](#)]

**Disclaimer/Publisher’s Note:** The statements, opinions and data contained in all publications are solely those of the individual author(s) and contributor(s) and not of MDPI and/or the editor(s). MDPI and/or the editor(s) disclaim responsibility for any injury to people or property resulting from any ideas, methods, instructions or products referred to in the content.